

A Hybrid Numerical Analysis Method for Structural Health Monitoring

Scott C. Forth¹ and Alexander Staroselsky²

Summary

A new hybrid surface-integral-finite-element numerical scheme has been developed to model a three-dimensional crack propagating through a thin, multi-layered coating. The finite element method was used to model the physical state of the coating (far field), and the surface integral method was used to model the fatigue crack growth. The two formulations are coupled through the need to satisfy boundary conditions on the crack surface and the external boundary. The coupling is sufficiently weak that the surface integral mesh of the crack surface and the finite element mesh of the uncracked volume can be set up independently. Thus when modeling crack growth, the finite element mesh can remain fixed for the duration of the simulation as the crack mesh is advanced. This method was implemented to evaluate the feasibility of fabricating a structural health monitoring system for real-time detection of surface cracks propagating in engine components. In this work, the authors formulate the hybrid surface-integral-finite-element method and discuss the mechanical issues of implementing a structural health monitoring system in an aircraft engine environment.

Introduction

Most field failure issues of components can be traced back to design, manufacturing, repair and inspection processes or unidentified usage conditions. In severe cases, these conditions can cause fatigue cracks to initiate and propagate, sometimes undetected, through the part causing catastrophic failure. Fortunately, most of these cracks are detected through routine inspection and overhaul. However, there are instances where abnormalities in the manufacturing process can cause undetectable imperfections that may produce fatigue cracks in the fielded part. Therefore, use of structural health monitoring systems capable of detecting impending failures would allow timely maintenance actions to increase overall safety. The economic impact of such a system is tremendous, based on four principal effects: (i) reducing the inventory, (ii) reducing maintenance cost, (iii) extending life of structures by condition based maintenance, and (iv) market advantage.

In this paper, the authors develop an effective numerical procedure to solve spatial problems of crack propagation in heterogeneous media and propose a structural health monitoring system. Work focuses on the development of a hybrid numerical method to analyze a crack propagating through a thin, multi-layer coated part. The primary objective of the hybrid method is to combine the advantages of finite elements and boundary elements to predict three-dimensional crack propagation. The finite element method (FEM) was used to model the state of the part (far field), and the surface integral method (SIM) was used to model the fatigue crack growth. A key advantage of this approach is that only the crack surfaces have to be re-meshed during crack propagation, with the FEM remaining the same.

The authors further propose a structural health monitoring system that operates by detecting a change in the electrical impedance of a conductive mesh due to mechanical changes caused by cracks.

¹ Mechanics & Durability Branch, NASA Langley Research Center, MS 188E, 2 W. Reid St., Hampton, VA 23681

² United Technologies Research Center, MS 129-73, 411 Silver Lane, E. Hartford, CT 06108

The model crack sensor consists of three layers deposited sequentially onto the surface of the component, as shown in Figure 1. The first insulating layer is deposited directly onto the component to electrically isolate a conductive mesh from the part. The second layer consists of a metallic wire grid deposited over the insulating layer. Finally, a protective topcoat is deposited over the metallic grid to protect it from oxidative or chemical attack, as well as to protect the grid from electrical interference due to conductive particle contamination. Cracks propagating at the component surface will fracture the grid resulting in impedance changes of the grid that will be detected by a sensor electronics package. The spatial separation between wires determines the crack size resolution the mesh can detect.

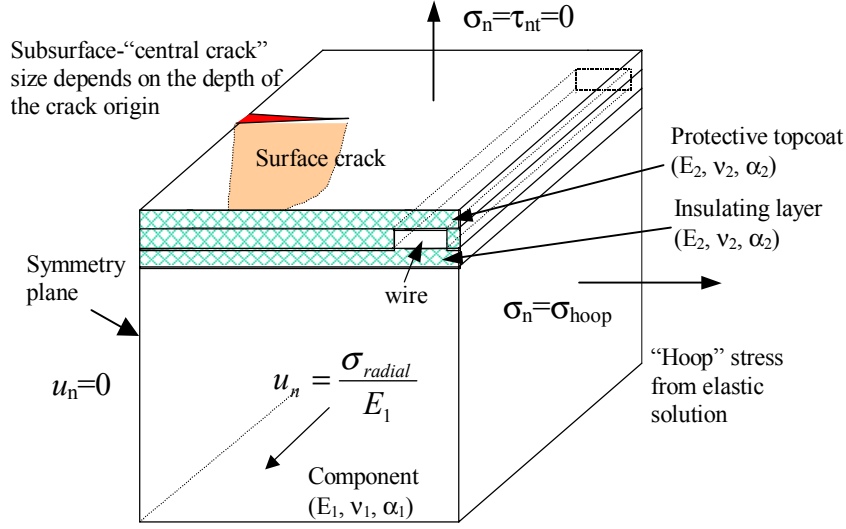


Figure 1: 3D problem formulation - geometry and loading conditions.

Formulation of the Numerical Method

The surface integral method is an indirect boundary element method based on the superposition of force multipoles to represent two-[1, 2] and three-dimensional [3, 4, 5] fractures. The tractions induced by a fracture can thus be represented by the integral equation

$$t_k = \iint_A \Gamma_{kmn} n_m \delta_n dA \quad (1)$$

where t_k is the traction vector, A is the surface area of the nonplanar fracture, Γ_{kmn} is the stress influence function, n_m is the normal to the fracture surface, and δ_n represents variations of crack displacement where δ_1 is crack opening, and δ_2, δ_3 are orthogonal components of crack shear. The stress influence function used in this formulation was obtained by differentiating Rongved's fundamental solution [6] for point forces near a planar bimaterial interface.

Traction boundary conditions are enforced at collocation points located at the element centroids of a piecewise planar representation of the fracture. In the vicinity of a collocation point, one can subtract

off the integral equivalent of a rigid body displacement to reduce the order of the singularity that can be integrated in the Cauchy principal-value sense. Discretization of the fracture surface into crack elements leads to the following equivalent form of the traction equation

$$t_k = \sum_{\substack{i=1 \\ i \neq q}}^{Nele} \iint_{A_i} \Gamma_{kmn} n_m^q h_n \hat{\delta}_n^i dA + \iint_{A_q} \Gamma_{kmn} n_m^q (h_n - I_n) \hat{\delta}_n^q dA + \oint_{A_q} \bar{N}^q \cdot \bar{\nabla} \phi_{kn} \hat{\delta}_n^q dS \quad (2)$$

where $Nele$ is the number of elements, the superscript i indicates crack element correspondence, q identifies the singular crack element containing the collocation point, h is the local interpolation function defined such that the near-tip displacements vary as the square root of the perpendicular distance from the crack front, A_i is the surface area of the i th crack element, N is the outward unit normal to the contour enclosing A_q , and it follows from Green's Lemma that $\Gamma_{kmn} n_m^q = \bar{\nabla} \cdot \bar{\nabla} \phi_{kn}$ where Γ_{kmn} and ϕ_{kn} are continuously differentiable along the closed contour. Using shorthand notation, equation (2) can be rewritten as

$$\{t\} = [C] \{\hat{\delta}\} \quad (3)$$

where C_{kn} represents the coefficient matrix. A full derivation of the governing equations can be found in Forth and Keat (1996) [4].

The combination of the surface integral method with the finite element method has been accomplished for two- [2] and three-dimensional [7] fracture analyses using superposition. The two constitutive models are coupled through the need to satisfy boundary conditions on the external boundary and crack surface. The formulation of the finite element equations is well documented, and can be presented in shorthand notation as

$$[K] \{U^{FE}\} = \{R\} - \{R^C\} \quad (4)$$

where $[K]$ is the finite element stiffness matrix, $\{U^{FE}\}$ is the vector of finite element nodal displacements, $\{R\}$ is the external nodal load vector, and $\{R^C\}$ is introduced to the equation to satisfy the external traction boundary conditions that are not enforced in the surface integral model. $\{R^C\}$ can be defined with respect to the surface integral crack opening displacement vector such that

$$\{R^C\} = [G] \{\hat{\delta}\} \quad (5)$$

where $[G]$ is derived such that the nodal forces are statically equivalent to the surface integral tractions acting on the external surface patches.

The traction equation for the surface integral method, as defined in equation (3), then can be modified to accommodate the finite element correction $\{t^C\}$ at the crack.

$$[C] \{\hat{\delta}\} = \{t\} - \{t^C\} \quad (6)$$

$\{t^C\}$ can then be expressed in terms of the finite element nodal displacements such that

$$\{t^C\} = [S] \{U^{FE}\} \quad (7)$$

The complete system of equations can be written by combining equations (4), (5), (6) and (7) to obtain the following partitioned matrix equation

$$\begin{bmatrix} K & G \\ S & C \end{bmatrix} \begin{Bmatrix} U^{FE} \\ \hat{\delta} \end{Bmatrix} = \begin{Bmatrix} R \\ t \end{Bmatrix} \quad (8)$$

To impose displacement boundary conditions, the equation must be reformulated in terms of the total displacements $\{U^{TOT}\}$ as

$$\{U^{TOT}\} = \{U^{FE}\} + \{U^{SI}\} \quad (9)$$

where

$$\{U^{SI}\} = [L] \{\hat{\delta}\} \quad (10)$$

in which $[L]$ is computed with the displacement influence functions. Therefore, the final form of the hybrid governing integral equation can be written as

$$\begin{bmatrix} K & (G - KL) \\ S & (C - SL) \end{bmatrix} \begin{Bmatrix} U^{TOT} \\ \hat{\delta} \end{Bmatrix} = \begin{Bmatrix} R \\ t \end{Bmatrix} \quad (11)$$

Crack Propagation Model

Three-dimensional fracture models, such as the surface integral method, can make use of two-dimensional growth laws by applying them locally along the crack front. To propagate the crack, both the direction and extension must be computed at each crack tip element. The maximum circumferential stress theory [8] for direction, and the Forman fatigue crack growth equation [9], were applied here due to their wide industrial acceptance and ease of implementation. Maximum circumferential stress theory determines the direction of crack propagation, θ , by maximizing the circumferential stress at the crack tip such that:

$$K_I \sin \theta + K_{II} (3 \cos \theta - 1) = 0 \quad (12)$$

where θ is the angle of growth direction expressed in the local normal-tangential coordinate system of the tip element and K_I and K_{II} are the mode I and mode II stress intensity factors, respectively. The Forman equation was developed to curve fit a large material database that is available through NASA Johnson Space Center and is defined as:

$$\frac{da}{dN} = \frac{C(1-f)^n (\Delta K_{eq})^n \left(1 - \frac{\Delta K_{th}}{\Delta K_{eq}}\right)^p}{(1-R)^n \left(1 - \frac{\Delta K_{eq}}{(1-R)K_C}\right)^q} \quad (13)$$

where da/dN is the rate of crack growth based on crack length a and cycle count N ; R is the stress ratio $\sigma_{min}/\sigma_{max}$; ΔK_{eq} is the equivalent stress intensity factor range which for mixed-mode is defined to be $\Delta K_{eq} = \sqrt{(\Delta K_I)^2 + (\Delta K_{II})^2 + (\Delta K_{III})^2}$ in accordance with the mixed-mode definition of strain energy release rate [10]; C , n , p and q are empirically derived material constants; K_C is the fracture toughness; ΔK_{th} is the threshold stress intensity factor range and f is the crack opening function.

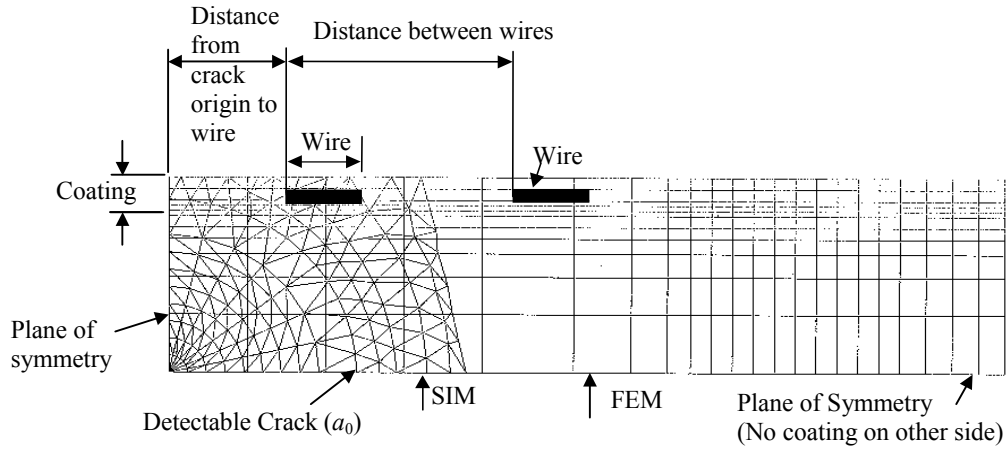


Figure 2. Hybrid Finite element mesh (FEM) and Surface integral mesh (SIM) to predict wired coating failure. Wires break as the crack in the part propagates.

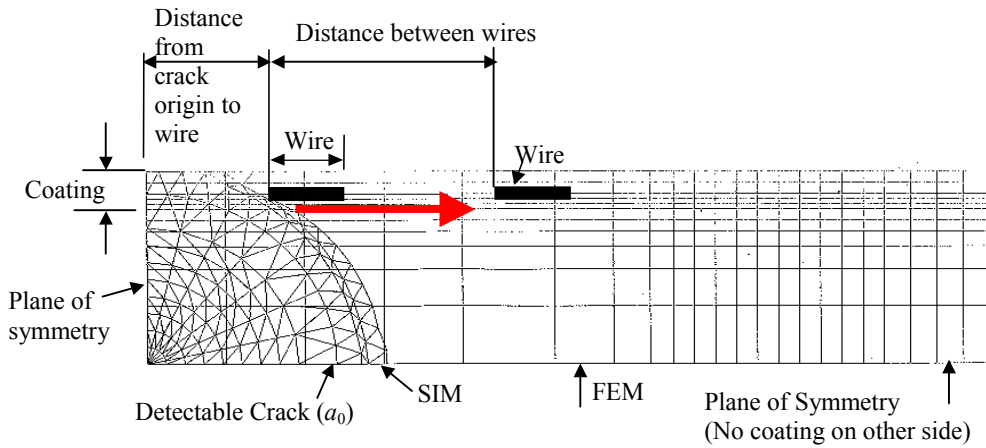


Figure 3. Hybrid Finite element mesh (FEM) and Surface integral mesh (SIM) to predict wired coating failure. Fracture of the coating system due to thickness and wire spacing.

Structural Health Monitoring System Analysis

The numerical model was comprised of 240 3D brick, 8-noded finite elements and 200 surface integral elements and the crack was propagated using material properties and loading conditions representative of an engine operating environment. The initial crack radius was defined as a_0 , the base material (E_1 , ν_1 , α_1) are Young's modulus, Poisson's ratio and coefficient of thermal expansion, respectively) and the wire mesh were assumed to be of the same material. In addition, the insulating and protective layers were assumed to have the same material properties (E_2 , ν_2 , α_2). The initial crack was located equi-distant between wires such that the wire spacing (s) would be minimized to detect a crack of size a_0 as it propagated. All spatial variables are non-dimensionalized to the initial crack length, a_0 , and material variables are non-dimensionalized to the component material (E_1 , ν_1 , α_1). Initially, the crack has a penny shape and is completely buried in the base material.

In this paper the authors numerically studied two crack propagation modes, specifically through-layer cracking (Fig. 2) and coating failure (Fig. 3). The insulating layer and protective top-coat are brittle, e.g. a lower fracture toughness, in comparison to the component material and will therefore fracture at a lower stress. The key factors in preventing fracture of the coating are the position and spacing of the wire in the mesh. Further details of this structural health monitoring system can be found in Forth and Staroselsky (2001) [11]. If the wire is placed too close to the surface, the insulating layer will simply fall off as the fatigue crack propagates through the part, while the wire remains intact. If the wire is placed too close to the part, then the fatigue crack will break through the insulating layer between the part and the wire causing delamination to occur at the interface. If the wires are spaced too far apart, a crack of size a_0 will not be detected. Therefore, the wire in the sensor must be embedded within the coating a minimum of 25% of the coating thickness from either surface to provide adequate structural integrity and electrical insulation between the component and wire. The wires must also be spaced a maximum of eighty percent of the predetermined detectable crack size, a_0 .

Conclusions

A novel hybrid numerical method to study three-dimensional crack propagation in a layered structure has been developed. This method combined with a crack propagation criterion made possible the study of incremental growth of three-dimensional non-planar cracks as well as to hypothesize the requirements for a structural health monitoring system. The fracture mechanics modeling has shown that it is feasible to design a patterned coating on an engine component which will be adherent at the stresses and temperatures normally present in engine operation, and will fracture in a controlled manner when there is an underlying crack in the part. The model has predicted an upper boundary for the total coating thickness, of which at least 25% of the coating thickness must be the protective layer covering the conductive grid, and a wire spacing of 80% of the predetermined detectable flaw size for the system to be structurally reliable.

Reference

- [1] Love, A.E.H. (1944): *A Treatise on Mathematical Theory of Elasticity*, Dover Pub., New York.
- [2] Annigeri, B.S. and Cleary, M.P. (1984): "Surface integral finite element hybrid (SIFEH) method for fracture mechanics," *Int. J. for Num. Meth. In Eng.*, Vol. 20, pp. 869-885.
- [3] Keat, W.D., Erguven, M.E. and Dwyer, J.F. (1996): "Modeling of 3D mixed-mode fractures near planar bimaterial interfaces using surface integrals," *Int. J. for Num. Meth.*, Vol. 39, pp.3679-3703.
- [4] Forth, S.C. and Keat, W.D. (1996): "Three-dimensional nonplanar fracture model using the surface integral method," *Int. J. of Fracture*, Vol. 77, No.3, pp. 243-262.
- [5] Forth, S.C. and Keat, W.D. (1997): "Nonplanar Crack Growth Using the Surface Integral Method," *ASME Gas Turbines & Power*, Vol. 119, No. 4, pp. 964-968.
- [6] Rongved, L. (1955): "Force at a point in the interior of a semi-infinite solid," *Proc. 2nd Midwestern Conf. On Solid Mech.*, pp. 1-13.
- [7] Keat, W.D., B.S. Annigeri, and Cleary, M.P. (1988): "Surface integral and finite element hybrid method for two and three dimensional fracture mechanics analysis," *Int. J. of Frac.*, Vol. 36, pp. 35-53.
- [8] Erdogan, F. and Sih, G.H. (1963): *ASME J. of Basic Eng.*, Vol. 89, pp. 159-525.
- [9] Forman, R.G., and Mettu, S.R. (1992): "Behavior of Surface and Corner Cracks Subjected to Tensile and Bending Loads in Ti-6Al-4V Alloy," *Fracture Mech.*, 22nd Symposium, Vol. 1, ASTM STP 1131, pp. 519-546.
- [10] Erdogan, F. (1983): "Stress Intensity Factors," *J. Appl. Mech.*, Vol. 50, pp. 992-1002.
- [11] Forth, S.C. and Staroselsky, A. (2001). "Fracture evaluation of in-situ sensors for high temperature applications," *Proc. 10th Int. Conf. Fracture*, in press.